

**This manuscript has been submitted for publication in Scientific Reports. Please note that, despite having undergone peer-review, the manuscript has yet to be formally accepted for publication. Subsequent versions of this manuscript may have slightly different content. If accepted, the final version of this manuscript will be available via the 'Peer-reviewed Publication DOI' link on the right-hand side of this webpage. Please feel free to contact any of the authors; we welcome feedback.**

# **Evaluating the decadal-to-centennial evolution of a new proxy-based NAO reconstruction during the Common Era**

Hernandez A<sup>1+\*</sup>, Sánchez-López G<sup>1+</sup>, Pla-Rabes S<sup>2</sup>, Comas-Bru L<sup>3</sup>, Parnell A<sup>4</sup>, Cahill N<sup>5</sup>, Geyer A<sup>1</sup>, Trigo R M<sup>6,7</sup>, Giralte S<sup>1</sup>.

<sup>1</sup>Institute of Earth Sciences Jaume Almera (ICTJA-CSIC), Barcelona, Spain

<sup>2</sup>CREAF, Campus de Bellaterra (UAB), Edifici C, 08193, Cerdanyola del Vallès

<sup>3</sup>School of Archaeology, Geography and Environmental Sciences, University of Reading, UK

<sup>4</sup>Hamilton Institute, Insight Centre for Data Analytics, Maynooth University, Kildare, Ireland

<sup>5</sup>Department of Mathematics and Statistics, Maynooth University, Maynooth, Kildare, Ireland.

<sup>6</sup>Instituto Dom Luiz (IDL), Faculdade de Ciências, Universidade de Lisboa, 1749-016, Lisboa, Portugal

<sup>7</sup>Departamento de Meteorologia, Universidade Federal do Rio de Janeiro, 21941-916, Rio de Janeiro, Brasil

+Both authors have contributed equally

\*Corresponding author: [ahernandez@ictja.csic.es](mailto:ahernandez@ictja.csic.es)

## **Abstract**

The North Atlantic Oscillation (NAO) is the major atmospheric mode ruling European climate variability during winter and its significance is underpinned by the number of recent studies aimed at reconstructing past NAO variability across different time scales and temporal resolutions. We present a new 2000-year multi-annual, proxy-based, local NAO impact reconstruction, with associated uncertainties, employing a Bayesian approach. This new local NAO reconstruction is focused on the Iberian Peninsula, a geographical area not included in previous NAO reconstructions despite being a widely used region for instrumental-based NAO measurements. We also assess the main forcing drivers in order to unveil any discrepancies with previously published NAO reconstructions. Results show that, on a decadal scale, a low number of sunspots correlate to low NAO values. The comparison with other previously published NAO reconstructions allows us to observe the variability of solar influence on the NAO across a latitudinal gradient according to the position of the employed archives. Moreover, we highlight the potential role of other North Atlantic modes of variability (i.e., East Atlantic pattern) on the non-stationary behaviour of the NAO through the Common Era, likely via solar impact.

**Keywords:** lacustrine sediments, NAO reconstruction, Iberian Peninsula, Bayesian model, palaeoclimate

## 1-Introduction

The North Atlantic Oscillation (NAO) exerts a strong influence on the climate of the North Atlantic sector at inter-annual time scales during the boreal winter (Hurrell, 1995; Hurrell et al., 2003; Pinto and Raible, 2012; Pozo-Vázquez et al., 2001). In particular, the importance of the NAO to explain European climate variability has encouraged a number of initiatives to produce NAO reconstructions across different timescales (e.g., Glueck and Stockton, 2001; Goodkin et al., 2008; Luterbacher et al., 2001; Michel et al., 2018; Olsen et al., 2012; Ortega et al., 2015; Rogers, 1984; Trouet et al., 2009). More recently, there is a growing interest to disentangle the relative controls resulting from external forcing mechanisms (e.g. solar, volcanic activity and/or greenhouse gases) and internal variability (e.g., ocean, atmosphere, sea ice) to develop reliable projections of its future evolution (e.g., Chiodo et al., 2019; Deser et al., 2017; Hall et al., 2017; Ineson et al., 2011; Scaife et al., 2014; Sjolte et al., 2018; Swingedouw et al., 2015).

NAO reconstructions are either established by instrumental data (i.e., atmospheric pressure data from meteorological stations or from reanalysis datasets (Jones et al., 1997; Luterbacher et al., 1999; Portis et al., 2001; Vinther et al., 2003) or atmospheric and meteorological conditions inferred from documentary records (e.g., logbooks, chronicles, correspondence) collected over the North Atlantic European sector (e.g., Barriopedro et al., 2014; Cornes et al., 2013; Küttel et al., 2010; Mellado-Cano et al., 2019; Wheeler et al., 2010). NAO reconstructions are often based on single (Appenzeller et al., 1998; Cook et al., 1998; Goodkin et al., 2008; Olsen et al., 2012) or multiple (Cullen et al., 2001; Glueck and Stockton, 2001; Ortega et al., 2015; Trouet et al., 2009) natural archives that are sensitive to climate variables controlled by the NAO pattern.

The NAO reconstructions available so far generally agree with each other as well as with instrumental NAO indices until as late as c. 1850 CE (Common Era). However, considerable discrepancies are evident further back in time (Pinto and Raible, 2012). Multiple factors have been put forward to account for these disagreements, ranging from the quality of instrumental data, chronological uncertainties, the use of diverse calibration periods, the rise of temperature linked to the anthropogenic climate change, differences in the sensitivity of the archives to climate variations and/or limitations on the stationary relationship assumed between the climate sensors and the NAO (Lehner et al., 2012; Michel et al., 2018; Schmutz et al., 2000; Sjolte et al., 2018; Timm et al., 2004; Wanner et al., 2001; Zorita and González-Rouco, 2002). The relatively large internal variability of the NAO has been commonly associated with its non-stationary behaviour (Lehner et al., 2012; Raible et al., 2006). More recently the amplitude of the internal variability has been ascribed to the influence of other North Atlantic modes of climate variability (i.e., the East Atlantic—EA— and Scandinavian—SCA—patterns) that would modulate the variations in the strength and location of the NAO dipole from annual to multidecadal scales (Comas-Bru and McDermott,

2014; Mellado-Cano et al., 2019; Moore and Renfrew, 2012). Another important contributor to reduce the discrepancies amongst NAO reconstructions is to use more accurate definitions (i.e., local impacts vs regional reconstructions). For instance, a regional NAO assembling a large set of sub-decadal data from different archives and localities could provide much better constrains (Cook et al., 2019; Ortega et al., 2015; Sjolte et al., 2018) (Fig. 1a). However, each of those data sources may be recording the sign in a different way and this would result in a smoothed NAO signal. Many studies use just one or two records (Baker et al., 2015; Faust et al., 2016; Olsen et al., 2012; Trouet et al., 2009) (Fig. 1a), which provide a more accurate (avoiding over-smoothing) yet spatially limited reconstruction of the (local) NAO impact.

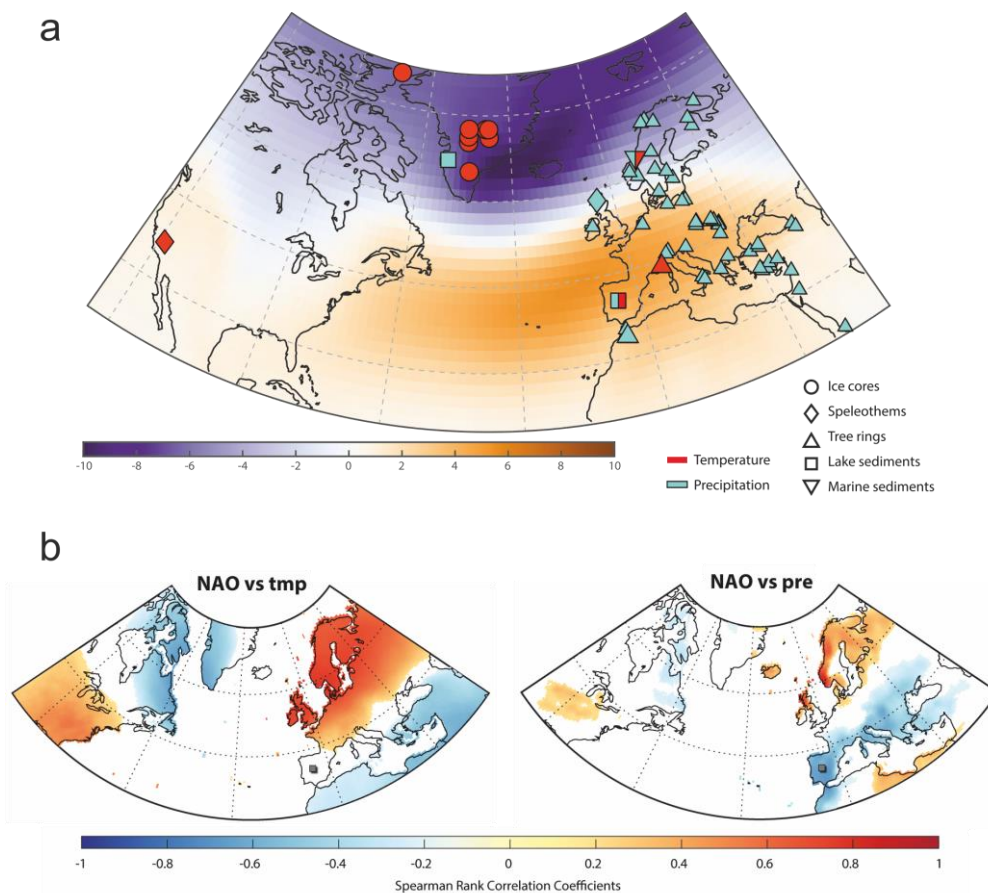


Fig.1. (a) Spatial display of the first eigenvector for the gridded winter (December – February) monthly sea-level pressure anomalies (in mb) for the North Atlantic domain—calculated using the Twentieth Century Reanalysis data set (20CRv2c; Compo et al., 2011). Location of the proxy-based records (ice cores, lake sediments, speleothems, tree rings, and marine sediments) employed in this study, using symbols and colours to represent the different types of archives and the reconstructed climate variables. (b) Correlation distribution maps between the winter precipitation and temperature (wPre and wTmp) datasets and the NAO, for the boreal winters (December – February) between 1901 and 2016, calculated using the CRU-TS4.1 global climate dataset (Harris et al., 2014) and the NAO and EA indices from Comas-Bru and Hernández (2018). Positive Spearman rank correlations are shown in red and negative correlations are shown in blue. Location of record used for NAO<sub>IP</sub> is indicated.

Although the impact of external forcing mechanisms on the NAO is still a matter of debate (Swingedouw et al., 2017), it has been traditionally assigned to the volcanic activity (Wanner et al., 2015), as seen by a predominance of positive NAO phases during periods of increased volcanic activity (Ortega et al., 2015; Sjolte et al., 2018). The role of solar activity, however, is even more controversial, with contradicting conclusions from proxy-based reconstructions (Brugnara et al., 2013; Faust et al., 2016; Ortega et al., 2015; Sjolte et al., 2018). Modelling (Chiodo et al., 2019; Woollings et al., 2010) and observational (Chiodo et al., 2012; Ineson et al., 2011) studies also display contradictory conclusions between the 11-year solar cycle and the NAO relationship (Chiodo et al., 2019; Thiéblemont et al., 2015). The studies arguing for a solar impact on the NAO do it through a "top-down" mechanism related to the ultraviolet irradiance pattern (Scaife et al., 2013). An increase of UV radiation during periods of high solar activity warm up the middle atmosphere leading to an altered stratospheric circulation that propagates pole- and down-wards to affect tropospheric jet streams and thus atmospheric circulation (Ineson et al., 2011; Martin-Puertas et al., 2012). However, the response of the NAO to the solar cycle would not occur immediately but rather after a lag of c. 3 years. This is because the impact of solar heating accumulates for several years in the ocean, and because of a positive feedback between the ocean and atmosphere (Gray et al., 2013; Scaife et al., 2013). Low sunspot activity results in a climate pattern very similar to the negative phase of the NAO (Lockwood, 2012) with longer lasting and more intense blocking episodes than during high solar blocking events (Barriopedro et al., 2008). A recent proxy-based study (Faust et al., 2016) further supports a linkage between the Grand minima of solar activity and negative NAO phases that accompany cooling events (e.g. Little Ice Age—LIA—) at decadal-to-centennial timescales.

NAO variability only accounts for c. 40 % of the climate variance that is ultimately captured by palaeorecords (Pinto and Raible, 2012), and on this basis a perfect NAO reconstruction is far from achievable beyond the instrumental period. For this, the interpretation of available NAO reconstructions requires a careful re-examination. The sensitivity of different climate archives to the NAO may vary at different spatio-temporal scales. This highlights the need to choose localities where the NAO impact on local climate is likely to be (more) stationary and to select paleo-sensors—the seasonality of which coincides to the season where the NAO's impact on climate is larger (Lehner et al., 2012; Ortega et al., 2015).

Lakes are highly sensitive to climate through changes in air temperature, wind speed, precipitation, and solar irradiance (Margalef, 1983). These climatic controls on lake and catchment processes impinge on the water properties of the lake and result in its sediments recording climate variability over timescales from seasonal to decadal (Blenckner et al., 2007; Catalan et al., 2013; Pla-Rabes and Catalan, 2011; Williamson et al., 2009). Because the NAO controls the variability of a wide range of climate-related variables (e.g.,

temperature, precipitation, wind-speed, solar radiation), sedimentary records capturing lake dynamics may integrate NAO variability better than a single local weather record (Hernández et al., 2015).

Most of these NAO reconstructions have been based on the use of some variant of regression models, often coupled with Principal Component Analysis (Michel et al., 2018). By contrast, richer models using Bayesian inference have been extensively used during the last decade for age-depth chronological building (Blaauw et al., 2007; Haslett and Parnell, 2008; Ramsey, 2008) as well as for climate and environmental reconstructions using biological proxies (Cahill et al., 2016; Haslett et al., 2006; Parnell et al., 2015; Tingley and Huybers, 2009). Nevertheless, neither Bayesian inference nor non-biological proxies have yet been used to reconstruct the NAO. The Bayesian approach holds a major advantage over traditional methods, as it is conceptually simpler to build a complex model which quantifies the relationship between multiple proxy and climate variables simultaneously—rather than relying on individual coefficients to describe the relationship (Birks et al., 2010; Li et al., 2010). Furthermore, it is possible to model observations under all conditions (i.e., modern analogues) (Guiot and de Vernal, 2007). In contrast, the price to be paid for "no modern analogue" situations means considerably larger uncertainties, which can be however, accounted for in the resulting reconstructions.

Here we present a quantitative reconstruction of the NAO for the central Iberian Peninsula (IP) over the last two millennia, along with its uncertainties, applying a Bayesian approach. We also assess the coherence between our new NAO reconstruction and previously published reconstructions from other locations, as well as potential external forcing mechanisms that would lead to disagreements between them as a result of the non-stationary spatial behaviour of the NAO.

## **2-DATA AND METHODS**

### **2.1-Proxy data**

We used the chemical composition of a lacustrine sediment core (CIM12-04A, 124.8 cm long) retrieved from an alpine lake located in the Central Iberian Range (Cimera Lake, 40°15'N – 5°18'W, 2140 m a.s.l.) (Sánchez-López et al., 2016). The chemical composition of the sediments was obtained by continuous X-ray fluorescence (XRF) analysis using the XRF Avaatech core scanner located at the University of Barcelona (Spain). The XRF settings (working conditions) were: 2 mm of spatial resolution, 2 mA, 15 s count times and 10 kV for lighter elements, with 55 s and 30 kV for heavier elements. Thirty chemical elements were measured, but only ten light (Al, Si, K, Ca, Ti, V, Cr, Mn, Fe and Zn) and three heavy (Rb, Sr and Zr) elements had enough counts to be considered robust.

The chronology of the sediment deposition of the CIM12-04A core have been previously determined by Sánchez-López et al., (2016). It was derived using the activity-depth profile of  $^{210}\text{Pb}$  in the uppermost 9 cm of the core together with six AMS  $^{14}\text{C}$  dating. The resulting model shows that sedimentary infill of Cimera Lake core spans from  $172 \pm 65$  BCE to 2012 CE (Sánchez-López et al., 2016).

## 2.2-Climate datasets

We used the NAO extended winter index (Jan-May) spanning the period 1824 – 2012 CE was employed to produce the NAO influence reconstruction. The data were obtained from the Climatic Research Unit (CRU) at the University of East Anglia (UK) (<https://crudata.uea.ac.uk/cru/data/pci.htm>). This NAO index was defined by Jones et al., (1997) and modified by Vinther et al., (2003). It was defined as the difference between the normalized monthly sea level pressure anomalies recorded at Reykjavik (Iceland) and those observed at Iberia (Gibraltar/Cadiz). Precipitation and temperature datasets employed for figures were obtained from CRU-TS4.01 (Harris et al., 2014), whereas NAO and EA data for figures were acquired from Comas-Bru and Hernández (2018).

## 2.3-Bayesian Model

We follow the Bayesian modelling approach of Parnell et al., (2016, 2015) to produce a reconstruction of NAO impact in the central IP. The relationship between proxy and climate is derived from a training data set for the instrumental/proxy calibration period and is expressed through a likelihood function. This function is combined with a prior probability density function containing parameter information to obtain a posterior probability distribution of the reconstructed NAO values using Bayes' theorem (Juggins and Birks, 2012). Whilst Parnell et al., (2015) based their framework on reconstructing multivariate temperature and moisture measurements from raw pollen data, the method is easily adaptable to other proxies and climate variables. Indeed, Cahill et al., (2016) used a similar approach to reconstruct sea level from foraminifera. In all cases the measures/counts of the proxy are required for a set of sediment layers (depths) in a core.

We summarize the mathematical details of the model in this section. Full technical details for the model fitting process are described in Parnell et al. (2015). We provide all the code used to create the reconstructions at [www.github.com/andrewcparnell/NAO](http://www.github.com/andrewcparnell/NAO).

The notation we use is as follows:

- $NAO(t)$  is the North Atlantic Oscillation value at time  $t$ . The goal of our model is to estimate  $NAO(t)$ , and its uncertainty, for a set of chosen times.

- $XRF_{ij}$  (expressed as counts per second) represents the chemical element  $j$  measured at a given depth  $i$  of the CIM12-04A core. We have  $i = 1, \dots, 647$  depths and  $j = 1, \dots, 13$  elements.
- We superscript both the quantities above with  $m$  and  $f$  so that  $XRF^m$  refers to the modern XRF data set, with associated known  $NAO^m$ , and  $XRF^f$  refers to the fossil data set, for which we wish to estimate  $NAO^f$ .
- $t_i$  refers to the age of the core at depth  $i$ . The ages in our core are all given in years BC/AD.
- $\theta$  refers to the set of parameters governing the relationship between the  $NAO$  and the  $XRF$  measurements, as well as the dynamics of how the  $NAO$  changes over time.

Our model proceeds by creating a Bayesian joint posterior distribution:

$$p(NAO^f, \theta | NAO^m, XRF^m, XRF^f) \propto p(XRF^f | NAO^f) \cdot p(XRF^m | NAO^m, \theta) \cdot p(NAO^f | \theta) \cdot p(\theta)$$

The term on the left-hand side of the equation is the posterior distribution and represents the probability distribution of fossil  $NAO$  impacts given the observed data. The terms on the right-hand side represent respectively, the likelihood (the probability distribution of  $XRF^f$  given  $NAO^f$ ), the distribution of  $XRF^m$  given  $NAO^m$ , and the prior distribution of the parameters governing the relationship between  $XRF$  and  $NAO$ .

For the distribution of  $XRF$  given  $NAO$ , we standardise all the  $XRF$  values (by chemical element) and fit a multivariate normal polynomial regression model (MVN). This means, for the values  $k = 1, \dots, 13$  chemical elements, we use:

$$[XRF_{i,1}, \dots, XRF_{i,13}] | NAO(t_i) \sim MVN(M_i, \Sigma)$$

where  $M_i = [\mu_{i,1}, \dots, \mu_{i,13}]$  with  $\mu_{ik} = \beta_{0k} + \beta_{1k} NAO(t_i) + \beta_{2k} NAO(t_i)^2$ , and  $\Sigma$  is a covariance matrix which captures the extra dependence between elements not explained by differences in  $NAO$ .

We set the prior distribution on  $NAO^f$  as a continuous-time random walk, which should reasonably match climate behaviour over the reconstructed time period (as in Haslett et al., (2006)). Other choices are available, such as long-memory or long-tailed stochastic processes Parnell et al., (2015) use a Normal inverse Gaussian process. Our prior distribution is:

$$NAO(t_i) \sim N(NAO(t_{i-1}), \sigma^2(t_i - t_{i-1}))$$

where  $\sigma^2$  is a parameter representing the variance 297 of the  $NAO^f$  increments for a unit of time.

Finally, we set uninformative prior distributions on the remaining parameters:

$$\beta_{0k}, \beta_{1k}, \beta_{2k} \sim N(0, 10), \sigma \sim U(0, 10), \Sigma^{-1} \sim \text{Wishart}(I_{13}, 14)$$

where  $N$  and  $U$  represent Normal and Uniform distributions and  $I$  is the identity matrix.

The above model is computationally expensive to fit using the default tools for Bayesian model fitting due to the large number of parameters and the high data dimension. Instead, as stated above, we follow the approach of Parnell et al. (Parnell et al., 2015), which involves a computational approximation to fit the model in three steps. The first step involves fitting the model to the modern data only. The second step involves estimating  $NAO^f$  for the fossil layers, and the third step involves constraining the estimated fossil  $NAO^f$  values according to a random walk model.

In the first step of the model, the total overlapping period between modern data, XRF proxy and observed NAO index (i.e.,  $NAO^m$  and  $XRF^m$ , respectively), extends from 1825 until 2012 AD. However, the XRF data from 1825 until 1930 AD has a lower resolution (i.e., decadal) than the 1930-2012 AD period, owing to the usual slight decrease in the age-depth model accuracy. Thus we restricted the overlapping fitting period employed in the analysis to 1930 – 2012 AD.  $XRF^m$  data were resampled with a yearly resolution for the overlapping period using the R function "approxTime" from the package "simecol" (Petzoldt and Rinke, 2007).

We fit the model in R (R Core Team, 2016) and use the JAGS software (Plummer, 2003) (Just Another Gibbs Sampler).

The performance of the fitting algorithm can be determined by looking at the Brooks-Gelman Rubin ( $\hat{R}$ ) statistic (Brooks and Gelman, 1998; Gelman and Rubin, 1992). We run the algorithm until all  $\hat{R}$  values are less than 1.05, which indicates satisfactory convergence of the algorithm to the posterior distribution.

We evaluate the performance of the model by testing the predictive performance of modern relationship between  $NAO^m$  and  $XRF^m$  (Step 1 as outlined above). We created predicted NAO values from the modern model using the modern NAO data (i.e, NAO index data). If the model is estimating NAO correctly there should be only 5% of observations outside the 95% interval, and 50% outside the 50% interval. Finally, the complete impact reconstruction is created using a 10-year time grid, and includes both 95% and 50% uncertainty intervals.

## 2.4-Statistical analyses

All NAO reconstructions have been converted to decadal time-scales to facilitate the comparison. For each reconstruction, all NAO values within the same decade have been averaged and we use that average value for its particular decade. The magnitude of the relationships between NAOs, sunspot numbers and volcanic eruptions were obtained according to Spearman's rank correlation coefficients ( $\rho$ ) and associated p values. Unless otherwise stated, significance (p-value) is always considered at values of  $p < 0.01$ . The statistical treatment of the data was performed with R software (R Core Team, 2017).

### 3-A new local NAO reconstruction: Central Iberian Peninsula

The NAO has a great effect on winter climate in the Iberian Peninsula (IP) (Comas-Bru and Hernández, 2018; Hernández et al., 2015; Trigo et al., 2008). In particular, high-mountain lakes from the IP are highly influenced by the NAO, because the cold and wet conditions during negative NAO phases control annual ice-cover dynamics (i.e., freezing and thawing) via the interaction between air temperature and precipitation (Sánchez-López et al., 2015). While the NAO is particularly relevant during the boreal winter, its impact on ecosystem and ice-cover dynamics is not restricted to this season (Gouveia et al., 2008); the NAO signal that is captured in lake records from this region spans from January to May (Sánchez-López et al., 2015).

A previous study (Sánchez-López et al., 2016) using geochemical and mineralogical data from the Cimera Lake record (40°15'N – 5°18'W, 2,140 m a.s.l.) revealed that climatic conditions, highly influenced by the NAO, are preserved in the sediments via the frequency of intense runoff episodes caused by rain-on-snow events as well as by lake productivity, which is primarily governed by the ice-cover duration. Here we use this data to reconstruct the NAO impact for the central IP ( $NAO_{IP}$ ) for the last two millennia using a Bayesian modelling approach (see Methods).

The reconstructed local NAO impact ranges between -2 and 2 and represents the quantitative impact of NAO for the central IP ( $NAO_{IP}$ ; Fig. 2). Only 2.9% of the observations fall outside the 95% confidence interval (Fig. 3). These results indicate satisfactory performance of the model and validate the  $NAO_{IP}$  reconstruction (see methods). The  $NAO_{IP}$  has not been reconstructed for the period c. 1200 – 1260 CE due to the lack of proxy data. Though the model permits such interpolation, the uncertainties would be too wide to enable any reasonable interpretation.

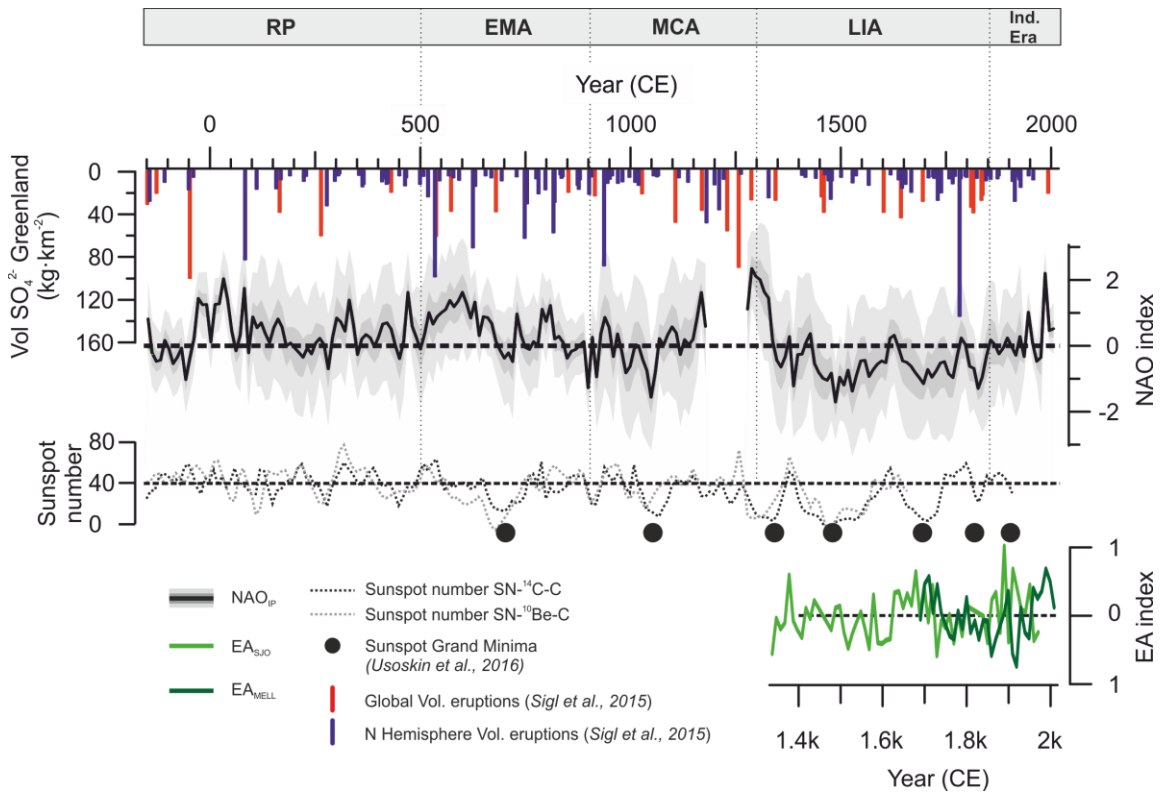


Fig.2: The NAO index data used in the fitting step of the model (thin black line), the median of the NAO impact for the Central Iberian Peninsula (NAO<sub>IP</sub>) obtained in this study (wide black line) and the 95% (light grey band) and 50% (dark grey band) uncertainty intervals.

The NAO<sub>IP</sub> shows multidecadal alternations between positive (> 0.5) and neutral (-0.5 to 0.5) phases of the NAO during the Roman Period (RP: ~200 BCE – 500 CE) (Fig. 2). Neutral to positive values characterize the first half of the RP period while there is a predominance of neutral values during the last half of the RP. During the Early Middle Ages (EMA: 500 – 900 CE) the NAO<sub>IP</sub> shows two cycles of positive-to-neutral and positive-to-negative (< -0.5) values. During the Medieval Climate Anomaly (MCA: 900 – 1300 CE), the NAO<sub>IP</sub> displays a trend from predominantly negative values to the most positive ones of the entire reconstruction. Negative NAO<sub>IP</sub> values clearly dominate the Little Ice Age (LIA: 1300 – 1850 CE) recording the most negative NAO<sub>IP</sub> values at ~1500 CE. In contrast, the Industrial Epoch (IE: 1850 – 2012 CE) shows a clear trend from neutral to positive values punctuated by large oscillations during the second half.

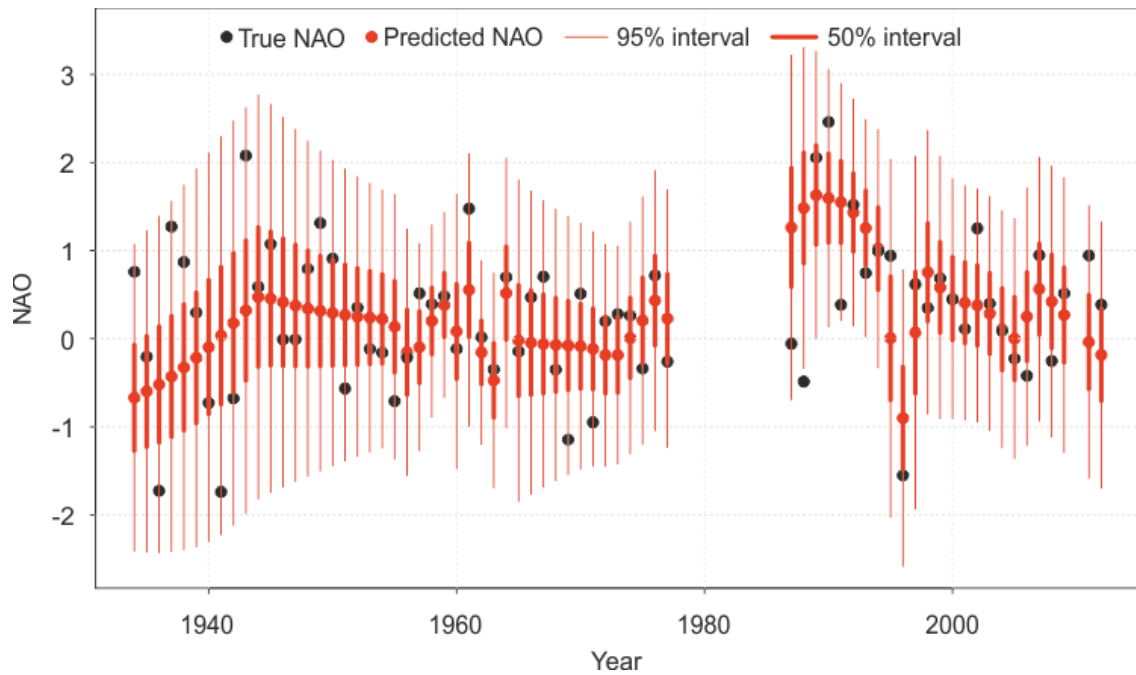


Fig.3: Black points correspond to true NAO data (i.e., NAO index data) and the red points show predicted median NAO impact values. The vertical red lines correspond to the 95% uncertainty interval (thin lines) and to the 50% uncertainty interval (wide lines), respectively.

#### 4-Comparison with previous NAO proxy-based records

The comparison between different proxy-based NAO reconstructions published in the last two decades (Table 1) points out a number of periods with consistent signals as well as some with notable differences (Fig. 4). All reconstructions show a similar long-term evolution with high positive NAO values during the MCA and lower positive or negative NAO values during the LIA (Fig. 4). This coherence across regions suggests an hemispheric imprint of this climate mode at low frequencies compared to the local impacts that might be recorded by each reconstruction over shorter timescales.

To establish the extent to which the multi-decadal variability between positive and negative excursions in  $NAO_{IP}$  during the last 2 ka compares to previously published reconstructions, we calculated Spearman's Rank Correlation Coefficients for decadal timescales (Table 2; Fig. 4). During the last 2 ka,  $NAO_{IP}$  displays the highest correlations with the W Europe mid-latitude records such as the NAO by Trouet et al., (2009;  $NAO_{TRO}$ ) ( $\rho = 0.51$ ;  $p < 0.01$ ;  $DF = 171$ ) and the NAO by Baker et al., (2015;  $NAO_{BAK}$ ) ( $\rho = 0.40$ ;  $p < 0.01$ ;  $DF = 206$ ). In contrast, the  $NAO_{IP}$  shows higher correlations with high-latitude and eastern records such as NAO by Ortega et al. (2015;  $NAO_{ORT}$ ) and NAO by Faust et al., (2016;  $NAO_{FAU}$ ) during the MCA ( $\rho = 0.84$ ;  $p < 0.01$ ;  $DF = 25$ ) and the IE ( $\rho = 0.94$ ;  $p < 0.01$ ;  $DF = 15$ ), respectively.

**Table 1: Previous NAO index reconstructions used in this work.**

<b>Authors</b>	<b>Reconstruction Period</b>	<b>Time Resolution</b>	<b>Predictors</b>	<b>Statistical Method</b>
Luterbacher et al. 2002 (NAO <sub>LUT</sub> )	1659-1995 CE 1500-1658 CE	Monthly Seasonal	Instrumental and proxy data predictors from Eurasia	Principal Component Regression (PCR)
Trouet et al. 2009 (NAO <sub>TRO</sub> )	c. 1050-2000 CE	Seasonal	Reconstructed winter precipitation for Scotland and February-to-June Palmer Drought Severity Index (PDSI) for Morocco	Normalised difference of the Scotland and Morocco records
Olsen et al. 2012 (NAO <sub>OLS</sub> )	c. 3250BCE - 1650 CE	Decadal	Paleo-redox proxy-based record of lake sediments from southwestern Greenland	3 <sup>rd</sup> component of a Principal Component Analysis (PCA) tuned by Monte-Carlo-Markov-Chain model (calibration based on Trouet et al. 2009)
Ortega et al. 2015 (NAO <sub>ORT</sub> )	c. 1050 - 2000 CE	Annual	Proxy data predictors (ice cores, lake sediment, speleothem and tree ring) from around the North Atlantic (Greenland, Europe, North America and North Africa)	Ensemble reconstruction of Principal Component Regressions (PCR)
Baker et al 2015 (NAO <sub>BAK</sub> )	1000BCE - 2000 CE	Annual	Speleothem	Principal Component Analysis (PCA)
Faust et al. 2016 (NAO <sub>FAU</sub> )	c. 800BCE - 1900 CE	Multiannual	Paleoproductivity (CaCO <sub>3</sub> and Ca/Si) proxy-based record of fjord sediments from Central Norway	Kernel smoother
Sjolte et al. 2018 (NAO <sub>SJO</sub> )	c. 1250 - 2000 CE	Seasonal	Reconstruction of atmospheric winter circulation for the North Atlantic region based on Greenland ice core records and a 1200-year-long simulation with an isotope-enabled climate model	Principal Component Analysis (PCA) supported by a Chi-square goodness-of-fit test
Cook et al 2019 (NAO <sub>COOK</sub> )	910-2018 CE	Seasonal	Tree rings	Principal components regression

**Table 2: Spearman's Rank Correlation Coefficients between decadal (10 years) NAO<sub>IP</sub> and other NAO indices and proxy-based reconstructions employed to build up NAO indices. Note: <sup>a</sup>, <sup>b</sup>, <sup>c</sup>, <sup>d</sup> indicate correlations with p-val < 0.01, 0.01 < p-val < 0.05, 0.05 < p-val < 0.1 and p-val > 0.1, respectively.**

		NAO <sub>LUT</sub>	NAO <sub>TRO</sub>	NAO <sub>OLS</sub>	NAO <sub>ORT</sub>	NAO <sub>BAK</sub>	NAO <sub>FAU</sub>	NAO <sub>SJO</sub>	NAO <sub>COOK</sub>
NAO <sub>IP</sub>	CE (200 BCE - Present)	0.18 <sup>d</sup>	<b>0.51<sup>a</sup></b>	0.20 <sup>b</sup>	0.22 <sup>b</sup>	<b>0.40<sup>a</sup></b>	0.08 <sup>d</sup>	0.13 <sup>d</sup>	0.07 <sup>d</sup>
	RP (200 BCE – 500 CE)	-	-	0.24 <sup>d</sup>	-	0.30 <sup>b</sup>	0.19 <sup>d</sup>	-	-
	EMA (500 – 900 CE)	-	-	-0.31 <sup>c</sup>	-	0.18 <sup>d</sup>	-0.19 <sup>d</sup>	-	-
	MCA (900 – 1300 CE)	-	0.28 <sup>d</sup>	0.30 <sup>d</sup>	<b>0.84<sup>a</sup></b>	0.57 <sup>a</sup>	-0.05 <sup>d</sup>	0.50 <sup>d</sup>	-0.26 <sup>d</sup>
	LIA (1300 – 1850 CE)	-0.22 <sup>d</sup>	0.29 <sup>b</sup>	0.27 <sup>d</sup>	0.06 <sup>d</sup>	0.35 <sup>a</sup>	-0.33 <sup>b</sup>	0.13 <sup>d</sup>	0.10 <sup>d</sup>
	IE (1850 CE - Present)	0.36 <sup>d</sup>	0.11 <sup>d</sup>	-	0.17 <sup>d</sup>	0.27 <sup>d</sup>	<b>0.94<sup>a</sup></b>	0.01 <sup>d</sup>	0.28 <sup>d</sup>

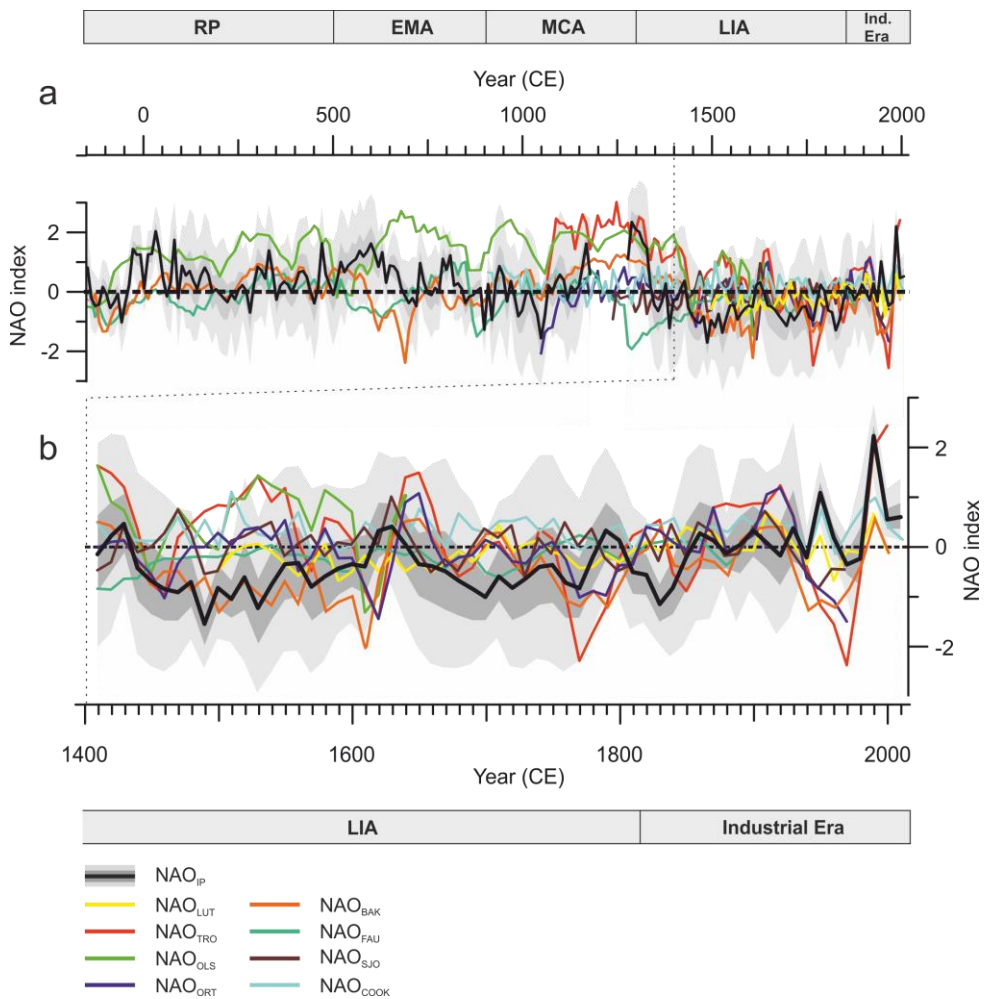


Fig.4: (a) Comparison of the NAO reconstructions for decadal timescales. (b) Magnified plots for the last six centuries.

The NAO<sub>IP</sub> shows larger differences with other NAO reconstructions during the earlier periods, that is, the RP and the EMA, with better agreement during the MCA, the LIA and the IE. The poor agreement during the RP and the EMA, corresponds to periods where the NAO<sub>IP</sub> displays values close to 0 with almost no negative values, whereas oscillations are much larger—either positive NAO by Olsen et al., (2012; NAO<sub>OLS</sub>) or negative (NAO<sub>BAK</sub> and

NAO<sub>FAU</sub>) —for those NAOs which cover these periods. These NAO differences might be attributed to the type, number, location and sensitivity of the archives used, the statistical approaches and external and/or internal forcings affecting each location in different ways.

Unlike gridded instrumental-based NAOs arising from datasets (e.g., atmospheric sea-level pressure) covering a vast geographical region (e.g., the North Atlantic region), the proxy-based NAO records are usually inferred using only a few climate proxies from restricted regions or locations (e.g., NAO<sub>TRO</sub>, NAO<sub>BAK</sub>, NAO by Sjolte et al., (2018; NAO<sub>SJO</sub>), or are based on a single paleorecord, as is the case of NAO<sub>OLS</sub>, NAO<sub>FAU</sub> and NAO<sub>IP</sub>. This restricted geographical constraint would imply that the reconstructed NAO signal is attributed to the local response of climate to this mode of variability rather than reflect a regional signal. Alternatively, the NAO by Cook et al., (2019; NAO<sub>COOK</sub>) NAO by Luterbacher et al., (2001; NAO<sub>LUT</sub>) and NAO<sub>ORT</sub> should be considered differently since they were reconstructed using a larger number of archives and have a wider spatial representation; i.e., a regional assemblage of local NAO impacts.

Nevertheless, we show here (Fig. 5) that the local impact of the NAO<sub>IP</sub> is capable of reflecting a much wider regional signal than what could be foreseen before. Thus, the reconstructed signal may be more accurate than in multi-archive reconstructions of regional NAOs. The reason for this is that the latter include different proxies from different archives that usually represent different seasons and climate variables, and, therefore, include a mixture of signals that will result in a smoother reconstruction.

Equally importantly, it is now clear that the NAO is far from unique in controlling the large-scale atmospheric variability in the North-Atlantic European region, acting simultaneously with other modes of variability that also play an important role in this region—namely the EA and SCA (Trigo et al., 2008). In particular, Comas-Bru and McDermott (Comas- Bru and McDermott, 2014) previously showed that different NAO/EA and NAO/SCA combinations influence European winter temperatures and precipitation as a consequence of sea level pressure (SLP) dipole migrations in the North Atlantic. In particular, this is expressed by a more homogeneous spatial pattern in temperature and precipitation over the IP for periods with a predominance of the same sign for both the NAO and the EA (i.e., MCA and LIA) than for periods when these modes are of opposite sign (i.e., RP and EMA) (Sánchez-López et al., 2016). It is noticeable that the geographical displacement of the northern centre of action of the North Atlantic SLP dipole is relatively smaller than the

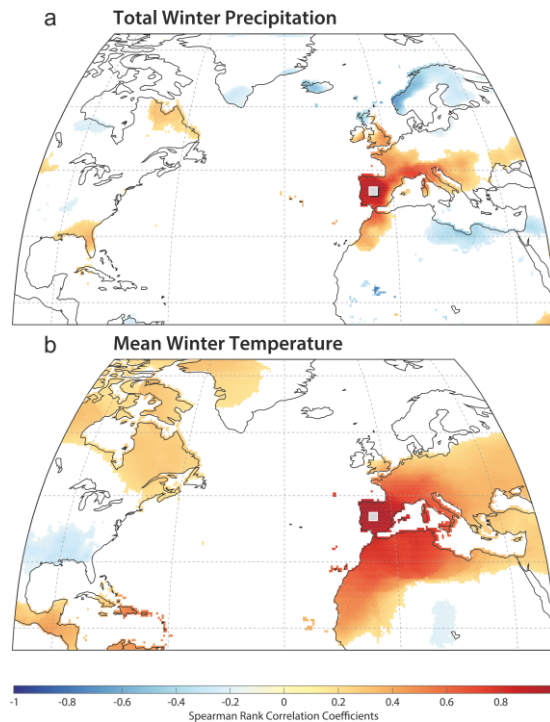


Fig 5. Correlation between winter (a) precipitation and (b) temperature at the site of  $NAO_{IP}$  (grey square) and each of the other grid cells to see how representative is the site for regional winter climate between 1901 and 2016, calculated using the CRU-TS4.1 global climate dataset (Harris et al., 2014). Positive Spearman rank correlations are shown in red and negative correlations are shown in blue.

concomitant migration of its southern pole during winters—where the NAO/EA have the same sign compared to years of opposite sign (Fig. 6). This could potentially explain the latitudinal variability observed for NAO reconstructions over the last millennia. Results also demonstrate that differences in precipitation between years of NAO and EA with the same and opposite signs (Fig. 7) are generally small for mid-latitudes (e.g., IP and Mediterranean basin) and larger for high-latitudes (e.g., Greenland, Ireland, and the UK). On the contrary, differences in temperature are larger for mid-latitudes and smaller for high-latitudes. These differences are almost inexistent in the western Atlantic sector (US and Canada) where the NAO impact is also significantly weaker. Hence, regional NAO reconstructions which use different archives (e.g., tree-rings, speleothems, ice-cores) recording different climate variables (e.g., precipitation, temperature) from different locations (high- vs mid-latitudes) could experience some kind of bias due to EA interactions.

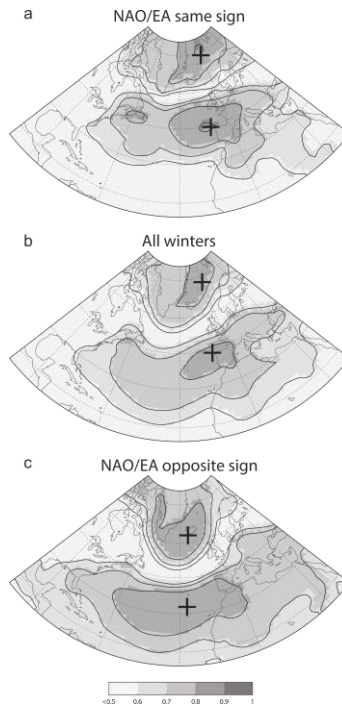


Fig.6: Teleconnectivity maps of the winter (DJF) monthly sea-level pressure field in the North Atlantic region for the period 1872 – 2009 and different linear combinations of the NAO-EA: a) winters with the NAO and the EA of the same sign; b) all winters; c) winters with the NAO and the EA of the opposite sign. Shaded areas represent Spearman correlations as per the colour bar. Black crosses indicate the location of the highest correlated grid cells. The NAO and the EA indices are the 1<sup>st</sup> and 2<sup>nd</sup> empirical orthogonal functions calculated from monthly SLP anomalies over a confined N. Atlantic sector using the Twentieth Century Reanalysis data set (20CRv2c; [Compo et al., 2011](#)).

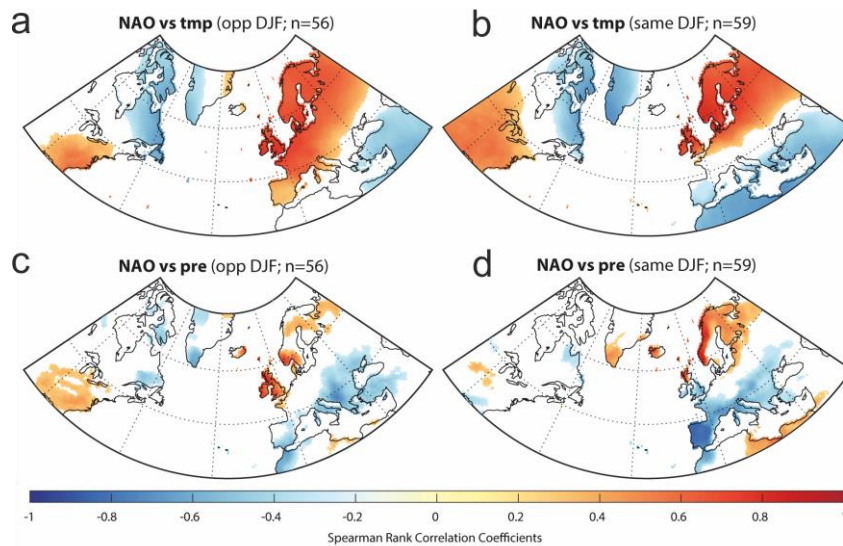


Fig. 7: Correlation distribution maps of winter NAO and (a,b) temperature and (c,d) precipitation. (a) and (c) are correlations for the subset of winters where NAO and EA are of opposite sign, whereas (b) and (d) are correlations for the subset of winters where NAO and EA are of the same sign. NAO and EA indices from [Comas-Bru and Hernandez \(2018\)](#) and climate data from the CRU-TS4.01 dataset ([Harris et al., 2014](#)). Location of NAO<sub>IP</sub> is shown as a grey square.

## 5-Volcanic eruption impact

Despite some previous proxy-based NAO reconstructions show a robust positive NAO response in the 4 – 5 years following the major eruptions of the last millennium (Ortega et al., 2015; Sjolte et al., 2018), a recent review of the impact of explosive volcanic eruptions on the main climate variability modes determined that no firm conclusions can be drawn at the moment (Swingedouw et al., 2017).

We compared  $NAO_{IP}$  with volcanic eruptions ( $n=42$ ) responsible for the largest accumulation of sulphate ( $> 20 \text{ kg}\cdot\text{km}^{-2}$ ) over Greenland according to Sigl et al., (2015) for the last 2 ka for decadal timescales (Table 3). We find positive reconstructed NAO values for c. 40% of the decades after these eruptions. This reinforces previous works (Ortega et al., 2015; Sjolte et al., 2018) that do not reach compelling conclusions on the relationship between NAO and volcanic activity. Nevertheless, if we relax the minimum emissions threshold and consider all Northern Hemispheric eruptions with an accumulation of sulphates larger than  $3 \text{ kg}\cdot\text{km}^{-2}$  ( $n = 93$ ), we find that decadal NAO values after these eruptions are positive in the 60% of the cases. Moreover, to explore the evolution of the volcanic impact on the  $NAO_{IP}$ , and its relationship with other external forcings (i.e., solar activity), the studied interval (150 BCE /Present) was divided into two millennial subperiods (higher/lower variance of solar activity): S1 (150 BCE – 1000 CE) and S2 (1000 – 2012 CE). Decades with positive values after NH eruptions during S1 ( $n = 52$ ) total 83%, whereas for S2 ( $n = 41$ ) this decreases to only 34%. Finally, if we compare the  $NAO_{IP}$  to decades with more than one eruption ( $n = 18$ ), we find that 72% of them reconstruct positive NAO values. This suggests that the sum of the eruptions has more impact than a single large eruption. A further comparison including all the NAO reconstructions shows a wide range of percentages (37 – 91%) of NAO+ decadal values agreeing with the largest NH volcanic eruptions (Table 3). Hence, there is an apparent influence from the occurrence of NH volcanic eruptions and the preferred signal of the NAO pattern over decadal timescales.

**Table 3: Percentage of positive NAO decades after the largest global (Sulfate accumulation in Greenland  $> 20 \text{ kg km}^{-2}$ ) and NH (Sulfate accumulation in Greenland  $> 3 \text{ Kg Km}^{-2}$ ) volcanic eruptions following Sigl et al (2015).**

	Global (150 BCE - 2012 CE)	NH (150 BCE -2012 CE)	NH (150 BCE -1000 CE)	NH (1000 - 2012 CE)	NH ( $n>1$ ) (150 BCE-2012 CE)
<b><math>NAO_{IP}</math></b>	<b>17/42 (40%)</b>	<b>56/93 (60%)</b>	<b>43/52 (83%)</b>	<b>14/41 (34%)</b>	<b>13/18 (72%)</b>
$NAO_{LUT}$	5/12 (42%)	10/27 (37%)	-	10/27 (37%)	4/7 (57%)
$NAO_{TRO}$	17/22 (77%)	28/44 (64%)	-	28/44 (64%)	5/9 (56%)
$NAO_{OLS}$	21/23 (91%)	50/55 (91%)	34/37 (92%)	16/18 (89%)	5/5 (100%)
$NAO_{ORT}$	11/22 (50%)	18/44 (41%)	-	18/44 (41%)	3/9 (33%)
$NAO_{BAK}$	24/46 (52%)	54/98 (55%)	32/52 (62%)	22/46 (48%)	7/18 (39%)
$NAO_{FAU}$	13/44 (30%)	38/94 (40%)	25/52 (48%)	12/42 (29%)	8/16 (50%)
$NAO_{SJO}$	8/18 (44%)	18/36 (50%)	-	18/36 (50%)	3/8 (13%)
$NAO_{COOK}$	22/27 (81%)	45/53 (85%)	6/7 (86%)	39/46 (85%)	11/11 (100%)

## 6-Solar forcing modulation

We also compared the  $NAO_{IP}$  with a decadal sunspot number reconstruction (Usoskin et al., 2016) through the CE. To avoid volcanic eruption interferences in the analysis, the decades corresponding to the fifteen largest volcanic eruptions globally were identified (Fig. 2 and Table S1) and, considered to be outliers, were removed from the solar forcing analysis.

The linear correlation between the decadal  $NAO_{IP}$  index and the sunspot number is non-significant ( $\rho = 0.20$ ;  $p > 0.1$ ;  $DF = 196$ ). However, the graphical representation of this relationship clearly displays an inflection point around the occurrence of 40 sunspots (Fig. 8). If we only consider sunspot numbers under 40, the linear correlation with  $NAO_{IP}$  becomes significant ( $\rho = 0.56$ ;  $p < 0.01$ ;  $DF = 103$ ). Additionally, to explore the stationarity of the solar influence on the NAO evolution, the studied interval (150 BCE – Present) was divided into the same two millennial subperiods considered previously: S1 (150 BCE – 1000 CE) and S2 (1000 – 2012 CE). The sunspot reconstruction during S1 displays fewer oscillations than during S2, and only includes one Grand solar minimum (Fig. 2).  $NAO_{IP}$  does not exhibit a significant correlation ( $\rho = 0.29$ ) for this period (S1). In contrast, during the S2, the sunspot

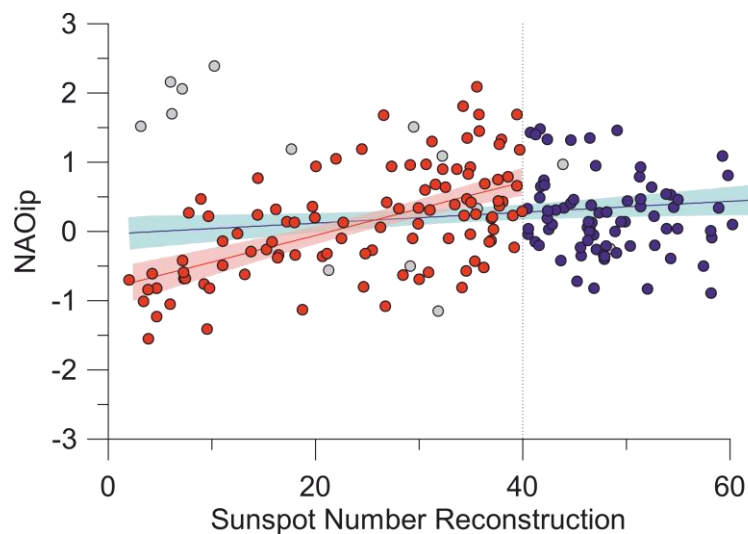


Fig. 8:  $NAO_{IP}$  values versus sunspot number reconstruction. Red dots represent samples with sunspot number values below 40, whereas blue dots indicate samples with sunspot number values above 40. Grey dots correspond to samples during decades with high volcanic eruptions and they have not been considered in the correlation analysis. Red line indicates linear correlation between NAO and Sunspot number ( $< 40$ ) and blue line for all data. Dotted line delimits samples with sunspot number values below and above 40.

exhibits a more oscillatory pattern with up to six reconstructed grand solar minima (Fig. 2). For this period, the  $NAO_{IP}$  vs Sunspot present a correlation value of  $\rho = 0.58$ ;  $p < 0.01$ ;  $DF = 46$  (Fig. 2 and 8; Table 4). This correlation is evident in the last 600 years (Fig. 2), where the  $NAO_{IP}$  shows a good agreement with the three latest Grand solar minima (i.e., Spörer, Maunder, and Dalton).

**Table 4: Spearman’s rank correlations coefficients between proxy-based NAO reconstructions and Sunspot Number reconstruction. Decades with important volcanic eruptions have been removed from the analysis. In bold, significant correlation values at 0.01 significance. Note that NAO<sub>TRO</sub> from Morocco is included to highlight the solar activity impact in lower latitudes.**

	SSN (150 BCE - 2012 CE)	SSN<40 (150 BCE - 2012 CE)	SSN<40 (150 BCE - 1000 CE)	SSN<40 (1000 - 2012 CE)
<b>NAO<sub>IP</sub></b>	0.20	<b>0.56</b>	0.29	<b>0.58</b>
NAO <sub>LUT</sub>	0.01	0.28	-	0.28
NAO <sub>TRO</sub>	0.06	<b>0.49</b>	-	<b>0.49</b>
<i>NAO<sub>TRO</sub> (Morocco)</i>	<i>0.15</i>	<b>0.42</b>	-	<b>0.42</b>
NAO <sub>OLS</sub>	0.08	0.03	<b>0.40</b>	0.21
NAO <sub>ORT</sub>	0.19	0.06	-	0.06
NAO <sub>BAK</sub>	0.06	0.23	<b>0.41</b>	0.36
NAO <sub>FAU</sub>	0.24	0.23	0.01	0.38
NAO <sub>SJO</sub>	0.18	0.02	-	0.02
NAO <sub>COOK</sub>	-0.09	0.01	-	-0.07

To evaluate this relationship, we have reproduced the same analysis with all the NAO reconstructions (Table 4 and Fig. S1). Results are similar to those obtained for the NAO<sub>ip</sub> exhibiting no significant correlations for the unfiltered data (i.e., using all sunspot numbers). However, the sunspot numbers under 40 also present a tipping point (Fig. S1) for those proxy-based NAO reconstructions where mid-latitudes records have a prevailing role (e.g., NAO<sub>IP</sub> and NAO<sub>TRO</sub>). In these cases, there is also a correlation between the decadal NAO values and the sunspot number ( $\rho > 0.40$ ;  $p < 0.01$ ;  $DF > 48$ ). To test whether the NAO behaviour is indeed significantly influenced by solar activity for sunspot numbers below 40 for reconstructions based on lower latitude records, we have also compared the southernmost record of the NAO<sub>TRO</sub>—Palmer Drought Severity Index (PDSI) based on tree ring data from Morocco (Esper et al., 2007)—with the sunspot number. This comparison confirms a significant correlation ( $\rho = 0.42$ ;  $p < 0.01$ ;  $DF = 48$ ) between the solar activity and NAO for mid-latitudes. These latitudinal differences of solar activity impact can be attributed, among other criteria previously exposed (e.g., type of proxy and methodology), to the fact that the solar variability signal is not uniformly distributed (Lean, 2017). Annual and decadal variations in solar activity have the largest impacts in the mid-latitudes (Haigh, 2011). Previous analyses of surface air temperatures (Lean and Rind, 2008) have already shown preferential warming in regions approximately in the range 30 – 60° latitude for both hemispheres.

## 7-Discussion and conclusions

This study presents a new multi-annual proxy-based NAO reconstruction using a Bayesian approach. This NAO reconstruction is compared to other available proxy-based reconstructions to review the NAO changes during the Common Era over these timescales, as well as their associated driving mechanisms. This comparison confirms there to be latitudinal complexity of the NAO with a puzzling interaction of several forcing factors.

There is an evident historical disagreement between all the available proxy-based reconstructions for the Common Era. While there is clear consensus for a mostly prevailing negative NAO phase during the Little Ice Age and positive one for the Medieval Climate Anomaly over centennial timescales, discrepancies emerge when NAO variability is analysed at shorter timescales. The same occurs in our attempt to identify patterns for the previous millennium (0 – 1000 CE) due to the scarcity of NAO reconstructions at multi-annual to decadal resolutions. We suggest oscillation of the NAO during the Roman Period (~ 200 BCE – 500 CE) dominated by positive and neutral phases, and two cycles from positive-to-neutral and positive-to-negative values during the Early Middle Ages (500 – 900 CE), although these oscillations are not coherent with other NAO reconstructions.

To disentangle the reasons underpinning the observed disagreements between the NAO reconstructions throughout time, we analysed their regional distribution and the available records, as well as the distinct impact of potential external forcings (i.e., volcanic eruptions and solar activity).

Our results demonstrate a latitudinal solar activity impact on the NAO variability over decadal timescales. The NAO reconstructions based on proxy records from mid-latitudes display significant positive correlations with the sunspot number, but this relationship is only found up to a certain solar activity threshold (number of sunspots = 40), after which the NAO index appears to be less influenced by solar activity. On the contrary, the impact of volcanic eruptions on the NAO is less clear, with a wide range of percentages showing dominant positive NAO values after large volcanic eruptions (or not).

Besides the influence of these two external forcing mechanisms we also assessed the role of an internal mechanism—namely the interaction of NAO with the second most important large-scale pattern of atmospheric circulation in the North-Atlantic European sector, i.e., the Eastern Atlantic (EA) pattern. It is well known that combinations of NAO and EA phases can change the geographical position of the NAO centres of action and affect the strength and latitudinal location of the dominant westerlies entering Europe from the Atlantic. As a consequence of this differential NAO impact on these climate variables according to the state of the EA, the chosen proxy and its location are crucial to more accurately reconstruct the NAO. Moreover, we are firmly convinced that this differential NAO impact could explain the differences between the available NAO reconstructions according to the geographical location of their proxies, the selected time intervals and the climate variables that they are

sensitive to. Although a wide regional distribution of records could apparently yield better results, the antagonistic impact of the combined NAO and EA modes on some climate variables over the mid- and high-latitude records could be masking or, even, cancelling out the actual NAO pattern.

It appears obvious that further studies are required to better understand the NAO's behaviour and the disagreements between the continuously increasing number of available NAO reconstructions. Regional NAO reconstructions like the ones derived by integrating a grid of instrumental or proxy-based regional data can be considered more robust—and can aid the understanding of general climate dynamics—only if the records employed are sensitive to the same forcing and therefore can capture the same signal. In contrast, local NAO reconstructions would be more useful to determine NAO impacts of local meteorological variables, which in turn influence the local ecosystems (and natural archives), economy, and society. Therefore, local NAO reconstructions can help to develop better mitigation policies against problems derived from NAO climatic effects such as agricultural yield or water scarcity. We also argue that new applied statistical approaches (i.e., Bayesian) would help to improve the reliability of the results. Overall, we stand for a more adaptable concept of proxy-based NAO using appropriate distinctions, since it is impossible to understand the NAO as a single pattern. Rather, it should be regarded as complex system that is controlled by multiple factors, some of which are stochastic and are therefore difficult to constrain.

## **Acknowledgements**

This work was financed by the Spanish Ministry of Economy and Competitiveness through the PaleoNAO (CGL2010-15767/BTE), RapidNAO (CGL2013-40608-R), and PaleoModes (CGL2016-75281-C2-1-R) projects and a PhD JAE grant (BOE 03/02/2011) for G.S.L. from the Spanish National Research Council (CSIC). A.H. is supported by a Beatriu de Pinós – Marie Curie Cofund programme fellowship (2016 BP 00023). A.G. is grateful for her Ramón y Cajal contract (RYC-2012-11024) and the MINECO grant VOLCLIMA (CGL2015-72629-EXP). A.P.'s work was supported by a Science Foundation Ireland Career Development Award grant 17/CDA/4695 and an SFI centre grant 12/RC/2289\_P2. R.M.T. was supported by the Portuguese FCT project: HOLMDRIVE—North Atlantic Atmospheric Patterns Influence on Western Iberia Climate: From the Late Glacial to the Present (PTDC/CTA-GEO/29029/2017).

## **Author Contributions**

A.H., G.S.L., S.P.R., and S.G. conceived the study. G.S.L., A.P., and N.C. constructed the model. A.H., S.P.R., and L.C.B. analysed the data. A.H., G.S.L., and L.C.B. designed the figures. A.H. and G.S.L. wrote the paper. All of the authors reviewed the manuscript.

## References

- Appenzeller, C., Stocker, T.F., Anklin, M., 1998. North Atlantic Oscillation Dynamics Recorded in Greenland Ice Cores. *Science* 282, 446–449. <https://doi.org/10.1126/science.282.5388.446>
- Baker, A., Hellstrom, J.C., Kelly, B.F.J., Mariethoz, G., Trouet, V., 2015. A composite annual-resolution stalagmite record of North Atlantic climate over the last three millennia. *Sci. Rep.* 5, 1–8. <https://doi.org/10.1038/srep10307>
- Barriopedro, D., Gallego, D., Alvarez-Castro, M.C., García-Herrera, R., Wheeler, D., Pena-Ortiz, C., Barbosa, S.M., 2014. Witnessing North Atlantic westerlies variability from ships' logbooks (1685–2008). *Clim. Dyn.* 43, 939–955.
- Barriopedro, D., García-Herrera, R., Huth, R., 2008. Solar modulation of Northern Hemisphere winter blocking. *J. Geophys. Res. Atmospheres* 113. <https://doi.org/10.1029/2008JD009789>
- Birks, H.J.B., Heiri, O., Seppä, H., Bjune, A.E., 2010. Strengths and Weaknesses of Quantitative Climate Reconstructions Based on Late-Quaternary. *Open Ecol. J.* 3.
- Blaauw, M., Bakker, R., Christen, J.A., Hall, V.A., Plicht, J. van der, 2007. A Bayesian Framework for Age Modeling of Radiocarbon-Dated Peat Deposits: Case Studies from the Netherlands. *Radiocarbon* 49, 357–367.
- Blenckner, T., Adrian, R., Livingstone, D.M., Jennings, E., Weyhenmeyer, G.A., George, D.G., Jankowski, T., Järvinen, M., Aonghusa, C.N., Nöges, T., Straile, D., Teubner, K., 2007. Large-scale climatic signatures in lakes across Europe: a meta-analysis. *Glob. Change Biol.* 13, 1314–1326. <https://doi.org/10.1111/j.1365-2486.2007.01364.x>
- Brooks, S.P., Gelman, A., 1998. General Methods for Monitoring Convergence of Iterative Simulations. *J. Comput. Graph. Stat.* 7, 434–455. <https://doi.org/10.1080/10618600.1998.10474787>
- Brugnara, Y., Brönnimann, S., Luterbacher, J., Rozanov, E., 2013. Influence of the sunspot cycle on the Northern Hemisphere wintertime circulation from long upper-air data sets. *Atmospheric Chem. Phys.* 13, 6275–6288. <https://doi.org/10.5194/acp-13-6275-2013>
- Cahill, N., Kemp, A.C., Horton, B.P., Parnell, A.C., 2016. A Bayesian hierarchical model for reconstructing relative sea level: from raw data to rates of change. *Clim. Past* 12, 525–542. <https://doi.org/10.5194/cp-12-525-2016>
- Catalan, J., Pla-Rabés, S., Wolfe, A.P., Smol, J.P., Rühland, K.M., Anderson, N.J., Kopáček, J., Stuchlík, E., Schmidt, R., Koinig, K.A., Camarero, L., Flower, R.J., Heiri, O., Kamenik, C., Korhola, A., Leavitt, P.R., Psenner, R., Renberg, I., 2013. Global change revealed by palaeolimnological records from remote lakes: a review. *J. Paleolimnol.* 49, 513–535. <https://doi.org/10.1007/s10933-013-9681-2>
- Chiodo, G., Calvo, N., Marsh, D.R., Garcia-Herrera, R., 2012. The 11 year solar cycle signal in transient simulations from the Whole Atmosphere Community Climate Model. *J. Geophys. Res. Atmospheres* 117. <https://doi.org/10.1029/2011JD016393>
- Chiodo, G., Oehrlein, J., Polvani, L.M., Fyfe, J.C., Smith, A.K., 2019. Insignificant influence of the 11-year solar cycle on the North Atlantic Oscillation. *Nat. Geosci.* 12, 94–99. <https://doi.org/10.1038/s41561-018-0293-3>
- Comas-Bru, L., Hernández, A., 2018. Reconciling North Atlantic climate modes: revised monthly indices for the East Atlantic and the Scandinavian patterns beyond the 20th century. *Earth Syst. Sci. Data* 10, 2329–2344. <https://doi.org/10.5194/essd-10-2329-2018>
- Comas-Bru, L., McDermott, F., 2014. Impacts of the EA and SCA patterns on the European twentieth century NAO–winter climate relationship. *Q. J. R. Meteorol. Soc.* 140, 354–363. <https://doi.org/10.1002/qj.2158>
- Cook, E.R., D'Arrigo, R.D., Briffa, K.R., 1998. A reconstruction of the North Atlantic Oscillation using tree-ring chronologies from North America and Europe. *The Holocene* 8, 9–17. <https://doi.org/10.1191/095968398677793725>
- Cook, E.R., Kushnir, Y., Smerdon, J.E., Williams, A.P., Anchukaitis, K.J., Wahl, E.R., 2019. A Euro-Mediterranean tree-ring reconstruction of the winter NAO index since 910 C.E. *Clim. Dyn.* 53, 1567–1580. <https://doi.org/10.1007/s00382-019-04696-2>
- Cornes, R.C., Jones, P.D., Briffa, K.R., Osborn, T.J., 2013. Estimates of the North Atlantic Oscillation back to 1692 using a Paris–London westerly index. *Int. J. Climatol.* 33, 228–248.
- Cullen, H.M., D'Arrigo, R.D., Cook, E.R., Mann, M.E., 2001. Multiproxy reconstructions of the North Atlantic Oscillation. *Paleoceanography* 16, 27–39. <https://doi.org/10.1029/1999PA000434>
- Deser, C., Hurrell, J.W., Phillips, A.S., 2017. The role of the North Atlantic Oscillation in European climate projections. *Clim. Dyn.* 49, 3141–3157. <https://doi.org/10.1007/s00382-016-3502-z>
- Esper, J., Frank, D., Büntgen, U., Verstege, A., Luterbacher, J., Xoplaki, E., 2007. Long-term drought severity variations in Morocco. *Geophys. Res. Lett.* 34. <https://doi.org/10.1029/2007GL030844>
- Faust, J.C., Fabian, K., Milzer, G., Giraudeau, J., Knies, J., 2016. Norwegian fjord sediments reveal NAO related winter temperature and precipitation changes of the past 2800 years. *Earth Planet. Sci. Lett.* 435, 84–93. <https://doi.org/10.1016/j.epsl.2015.12.003>
- Gelman, A., Rubin, D.B., 1992. Inference from Iterative Simulation Using Multiple Sequences. *Stat. Sci.* 7, 457–472.
- Glueck, M.F., Stockton, C.W., 2001. Reconstruction of the North Atlantic Oscillation, 1429–1983. *Int. J. Climatol.* 21, 1453–1465. <https://doi.org/10.1002/joc.684>
- Goodkin, N.F., Hughen, K.A., Doney, S.C., Curry, W.B., 2008. Increased multidecadal variability of the North Atlantic Oscillation since 1781. *Nat. Geosci.* 1, 844–848. <https://doi.org/10.1038/ngeo352>
- Gouveia, C., Trigo, R.M., DaCamara, C.C., Libonati, R., Pereira, J.M.C., 2008. The North Atlantic Oscillation and European vegetation dynamics. *Int. J. Climatol.* 28, 1835–1847. <https://doi.org/10.1002/joc.1682>

- Gray, L.J., Scaife, A.A., Mitchell, D.M., Osprey, S., Ineson, S., Hardiman, S., Butchart, N., Knight, J., Sutton, R., Kodera, K., 2013. A lagged response to the 11 year solar cycle in observed winter Atlantic/European weather patterns. *J. Geophys. Res. Atmospheres* 118, 13,405–13,420.
- Guiot, J., de Vernal, A., 2007. Chapter Thirteen Transfer Functions: Methods for Quantitative Paleoceanography Based on Microfossils, in: Hillaire-Marcel, C., De Vernal, A. (Eds.), *Developments in Marine Geology, Proxies in Late Cenozoic Paleoceanography*. Elsevier, pp. 523–563. [https://doi.org/10.1016/S1572-5480\(07\)01018-4](https://doi.org/10.1016/S1572-5480(07)01018-4)
- Haigh, P.J., 2011. Solar influences on Climate 20.
- Hall, R.J., Scaife, A.A., Hanna, E., Jones, J.M., Erdélyi, R., 2017. Simple Statistical Probabilistic Forecasts of the Winter NAO. *Weather Forecast.* 32, 1585–1601. <https://doi.org/10.1175/WAF-D-16-0124.1>
- Harris, I., Jones, P.D., Osborn, T.J., Lister, D.H., 2014. Updated high-resolution grids of monthly climatic observations – the CRU TS3.10 Dataset. *Int. J. Climatol.* 34, 623–642. <https://doi.org/10.1002/joc.3711>
- Haslett, J., Parnell, A., 2008. A Simple Monotone Process with Application to Radiocarbon-Dated Depth Chronologies. *J. R. Stat. Soc. Ser. C Appl. Stat.* 57, 399–418.
- Haslett, J., Whitley, M., Bhattacharya, S., Salter-Townshend, M., Wilson, S.P., Allen, J.R.M., Huntley, B., Mitchell, F.J.G., 2006. Bayesian palaeoclimate reconstruction. *J. R. Stat. Soc. Ser. A Stat. Soc.* 169, 395–438. <https://doi.org/10.1111/j.1467-985X.2006.00429.x>
- Hernández, A., Trigo, R.M., Pla-Rabes, S., Valero-Garcés, B.L., Jerez, S., Rico-Herrero, M., Vega, J.C., Jambrina-Enríquez, M., Giralt, S., 2015. Sensitivity of two Iberian lakes to North Atlantic atmospheric circulation modes. *Clim. Dyn.* 45, 3403–3417. <https://doi.org/10.1007/s00382-015-2547-8>
- Hurrell, J.W., 1995. Decadal Trends in the North Atlantic Oscillation: Regional Temperatures and Precipitation. *Science* 269, 676–679. <https://doi.org/10.1126/science.269.5224.676>
- Hurrell, J.W., Kushnir, Y., Ottersen, G., Visbeck, M., 2003. An Overview of the North Atlantic Oscillation, in: W, H.J., Y, K., G, O., M, V. (Eds.), *The North Atlantic Oscillation: Climatic Significance and Environmental Impact*. American Geophysical Union (AGU), Washington, US, pp. 1–35.
- Ineson, S., Scaife, A.A., Knight, J.R., Manners, J.C., Dunstone, N.J., Gray, L.J., Haigh, J.D., 2011. Solar forcing of winter climate variability in the Northern Hemisphere. *Nat. Geosci.* 4, 753–757. <https://doi.org/10.1038/ngeo1282>
- Jones, P.D., Jonsson, T., Wheeler, D., 1997. Extension to the North Atlantic oscillation using early instrumental pressure observations from Gibraltar and south-west Iceland. *Int. J. Climatol.* 17, 1433–1450. [https://doi.org/10.1002/\(SICI\)1097-0088\(19971115\)17:13<1433::AID-JOC203>3.0.CO;2-P](https://doi.org/10.1002/(SICI)1097-0088(19971115)17:13<1433::AID-JOC203>3.0.CO;2-P)
- Juggins, S., Birks, H.J.B., 2012. Quantitative Environmental Reconstructions from Biological Data, in: Birks, H.J.B., Lotter, A.F., Juggins, S., Smol, J.P. (Eds.), *Tracking Environmental Change Using Lake Sediments: Data Handling and Numerical Techniques, Developments in Paleoenvironmental Research*. Springer Netherlands, Dordrecht, pp. 431–494. [https://doi.org/10.1007/978-94-007-2745-8\\_14](https://doi.org/10.1007/978-94-007-2745-8_14)
- Küttel, M., Xoplaki, E., Gallego, D., Luterbacher, J., García-Herrera, R., Allan, R., Barriendos, M., Jones, P.D., Wheeler, D., Wanner, H., 2010. The importance of ship log data: reconstructing North Atlantic, European and Mediterranean sea level pressure fields back to 1750. *Clim. Dyn.* 34, 1115–1128. <https://doi.org/10.1007/s00382-009-0577-9>
- Lean, J.L., 2017. Sun-Climate Connections. *Oxf. Res. Encycl. Clim. Sci.* <https://doi.org/10.1093/acrefore/9780190228620.013.9>
- Lean, J.L., Rind, D.H., 2008. How natural and anthropogenic influences alter global and regional surface temperatures: 1889 to 2006. *Geophys. Res. Lett.* 35. <https://doi.org/10.1029/2008GL034864>
- Lehner, F., Raible, C.C., Stocker, T.F., 2012. Testing the robustness of a precipitation proxy-based North Atlantic Oscillation reconstruction. *Quat. Sci. Rev.* 45, 85–94. <https://doi.org/10.1016/j.quascirev.2012.04.025>
- Li, B., Nychka, D.W., Ammann, C.M., 2010. The Value of Multiproxy Reconstruction of Past Climate. *J. Am. Stat. Assoc.* 105, 883–895. <https://doi.org/10.1198/jasa.2010.ap09379>
- Lockwood, M., 2012. Solar Influence on Global and Regional Climates. *Surv. Geophys.* 33, 503–534. <https://doi.org/10.1007/s10712-012-9181-3>
- Luterbacher, J., Schmutz, C., Gyalistras, D., Xoplaki, E., Wanner, H., 1999. Reconstruction of monthly NAO and EU indices back to AD 1675. *Geophys. Res. Lett.* 26, 2745–2748. <https://doi.org/10.1029/1999GL900576>
- Luterbacher, J., Xoplaki, E., Dietrich, D., Jones, P.D., Davies, T.D., Portis, D., Gonzalez-Rouco, J.F., Storch, H. von, Gyalistras, D., Casty, C., Wanner, H., 2001. Extending North Atlantic oscillation reconstructions back to 1500. *Atmospheric Sci. Lett.* 2, 114–124. <https://doi.org/10.1006/asle.2002.0047>
- Margalef, R., 1983. *Limnología*. Omega, Barcelona, España.
- Martin-Puertas, C., Matthes, K., Brauer, A., Muscheler, R., Hansen, F., Petrick, C., Aldahan, A., Possnert, G., Geel, B. van, 2012. Regional atmospheric circulation shifts induced by a grand solar minimum. *Nat. Geosci.* 5, 397–401. <https://doi.org/10.1038/ngeo1460>
- Mellado-Cano, J., Barriopedro, D., García-Herrera, R., Trigo, R.M., Hernández, A., 2019. Examining the North Atlantic Oscillation, East Atlantic Pattern, and Jet Variability since 1685. *J. Clim.* 32, 6285–6298. <https://doi.org/10.1175/JCLI-D-19-0135.1>
- Michel, S., Swingedouw, D., Chavent, M., Ortega, P., Mignot, J., Khodri, M., 2018. Reconstructing climatic modes of variability from proxy records: sensitivity to the methodological approach. *Geosci. Model Dev. Discuss.* 1–48. <https://doi.org/10.5194/gmd-2018-211>
- Moore, G.W.K., Renfrew, I.A., 2012. Cold European winters: interplay between the NAO and the East Atlantic mode. *Atmospheric Sci. Lett.* 13, 1–8. <https://doi.org/10.1002/asl.356>

- Olsen, J., Anderson, N.J., Knudsen, M.F., 2012. Variability of the North Atlantic Oscillation over the past 5,200 years. *Nat. Geosci.* 5, 808–812. <https://doi.org/10.1038/ngeo1589>
- Ortega, P., Lehner, F., Swingedouw, D., Masson-Delmotte, V., Raible, C.C., Casado, M., Yiou, P., 2015. A model-tested North Atlantic Oscillation reconstruction for the past millennium. *Nature* 523, 71–74. <https://doi.org/10.1038/nature14518>
- Parnell, A.C., Haslett, J., Sweeney, J., Doan, T.K., Allen, J.R.M., Huntley, B., 2016. Joint palaeoclimate reconstruction from pollen data via forward models and climate histories. *Quat. Sci. Rev.* 151, 111–126. <https://doi.org/10.1016/j.quascirev.2016.09.007>
- Parnell, A.C., Sweeney, J., Doan, T.K., Salter-Townshend, M., Allen, J.R.M., Huntley, B., Haslett, J., 2015. Bayesian inference for palaeoclimate with time uncertainty and stochastic volatility. *J. R. Stat. Soc. Ser. C Appl. Stat.* 64, 115–138. <https://doi.org/10.1111/rssc.12065>
- Petzoldt, T., Rinke, K., 2007. simcol: An Object-Oriented Framework for Ecological Modeling in R. *J. Stat. Softw.* 22, 1–31. <https://doi.org/10.18637/jss.v022.i09>
- Pinto, J.G., Raible, C.C., 2012. Past and recent changes in the North Atlantic oscillation. *Wiley Interdiscip. Rev. Clim. Change* 3, 79–90. <https://doi.org/10.1002/wcc.150>
- Pla-Rabes, S., Catalan, J., 2011. Deciphering chrysophyte responses to climate seasonality. *J. Paleolimnol.* 46, 139. <https://doi.org/10.1007/s10933-011-9529-6>
- Plummer, M., 2003. JAGS: A program for analysis of Bayesian graphical models using Gibbs sampling. *Work. Pap.* 8.
- Portis, D.H., Walsh, J.E., El Hamly, M., Lamb, P.J., 2001. Seasonality of the North Atlantic oscillation. *J. Clim.* 14, 2069–2078.
- Pozo-Vázquez, D., Esteban-Parra, M.J., Rodrigo, F.S., Castro-Díez, Y., 2001. A study of NAO variability and its possible non-linear influences on European surface temperature. *Clim. Dyn.* 17, 701–715. <https://doi.org/10.1007/s003820000137>
- R Core Team, 2016. R: A language and environment for statistical computing. R Foundation for Statistical Computing, Vienna, Austria.
- Raible, C.C., Casty, C., Luterbacher, J., Pauling, A., Esper, J., Frank, D.C., Büntgen, U., Roesch, A.C., Tschuck, P., Wild, M., Vidale, P.-L., Schär, C., Wanner, H., 2006. Climate Variability-Observations, Reconstructions, and Model Simulations for the Atlantic-European and Alpine Region from 1500-2100 AD. *Clim. Change* 79, 9–29. <https://doi.org/10.1007/s10584-006-9061-2>
- Ramsey, C.B., 2008. Deposition models for chronological records. *Quat. Sci. Rev., INTegration of Ice-core, Marine and Terrestrial records (INTIMATE): Refining the record of the Last Glacial-Interglacial Transition* 27, 42–60. <https://doi.org/10.1016/j.quascirev.2007.01.019>
- Rogers, J.C., 1984. The Association between the North Atlantic Oscillation and the Southern Oscillation in the Northern Hemisphere. *Mon. Weather Rev.* 112, 1999–2015. [https://doi.org/10.1175/1520-0493\(1984\)112<1999:TABTNA>2.0.CO;2](https://doi.org/10.1175/1520-0493(1984)112<1999:TABTNA>2.0.CO;2)
- Sánchez-López, G., Hernández, A., Pla-Rabes, S., Toro, M., Granados, I., Sigró, J., Trigo, R.M., Rubio-Inglés, M.J., Camarero, L., Valero-Garcés, B., Giralt, S., 2015. The effects of the NAO on the ice phenology of Spanish alpine lakes. *Clim. Change* 130, 101–113. <https://doi.org/10.1007/s10584-015-1353-y>
- Sánchez-López, G., Hernández, A., Pla-Rabes, S., Trigo, R.M., Toro, M., Granados, I., Sáez, A., Masqué, P., Pueyo, J.J., Rubio-Inglés, M.J., Giralt, S., 2016. Climate reconstruction for the last two millennia in central Iberia: The role of East Atlantic (EA), North Atlantic Oscillation (NAO) and their interplay over the Iberian Peninsula. *Quat. Sci. Rev.* 149, 135–150. <https://doi.org/10.1016/j.quascirev.2016.07.021>
- Scaife, A.A., Arribas, A., Blockley, E., Brookshaw, A., Clark, R.T., Dunstone, N., Eade, R., Fereday, D., Folland, C.K., Gordon, M., Hermanson, L., Knight, J.R., Lea, D.J., MacLachlan, C., Maidens, A., Martin, M., Peterson, A.K., Smith, D., Vellinga, M., Wallace, E., Waters, J., Williams, A., 2014. Skillful long-range prediction of European and North American winters. *Geophys. Res. Lett.* 41, 2514–2519. <https://doi.org/10.1002/2014GL059637>
- Scaife, A.A., Ineson, S., Knight, J.R., Gray, L., Kodera, K., Smith, D.M., 2013. A mechanism for lagged North Atlantic climate response to solar variability. *Geophys. Res. Lett.* 40, 434–439. <https://doi.org/10.1002/grl.50099>
- Schmutz, C., Luterbacher, J., Gyalistras, D., Xoplaki, E., Wanner, H., 2000. Can we trust proxy-based NAO index reconstructions? *Geophys. Res. Lett.* 27, 1135–1138. <https://doi.org/10.1029/1999GL011045>
- Sigl, M., Winstrup, M., McConnell, J.R., Welten, K.C., Plunkett, G., Ludlow, F., Büntgen, U., Caffee, M., Chellman, N., Dahl-Jensen, D., Fischer, H., Kipfstuhl, S., Kostick, C., Maselli, O.J., Mekhaldi, F., Mulvaney, R., Muscheler, R., Pasteris, D.R., Pilcher, J.R., Salzer, M., Schüpbach, S., Steffensen, J.P., Vinther, B.M., Woodruff, T.E., 2015. Timing and climate forcing of volcanic eruptions for the past 2,500 years. *Nature* 523, 543–549. <https://doi.org/10.1038/nature14565>
- Sjolte, J., Sturm, C., Adolphi, F., Vinther, B.M., Werner, M., Lohmann, G., Muscheler, R., 2018. Solar and volcanic forcing of North Atlantic climate inferred from a process-based reconstruction. *Clim. Past* 14, 1179–1194. <https://doi.org/10.5194/cp-14-1179-2018>
- Swingedouw, D., Mignot, J., Ortega, P., Khodri, M., Menegoz, M., Cassou, C., Hanquiez, V., 2017. Impact of explosive volcanic eruptions on the main climate variability modes. *Glob. Planet. Change* 150, 24–45. <https://doi.org/10.1016/j.gloplacha.2017.01.006>
- Swingedouw, D., Ortega, P., Mignot, J., Guilyardi, E., Masson-Delmotte, V., Butler, P.G., Khodri, M., Séférian, R., 2015. Bidecadal North Atlantic ocean circulation variability controlled by timing of volcanic eruptions. *Nat. Commun.* 6, 1–12. <https://doi.org/10.1038/ncomms7545>

- Thiéblemont, R., Matthes, K., Omrani, N.-E., Kodera, K., Hansen, F., 2015. Solar forcing synchronizes decadal North Atlantic climate variability. *Nat. Commun.* 6, 8268. <https://doi.org/10.1038/ncomms9268>
- Timm, O., Ruprecht, E., Kleppek, S., 2004. Scale-dependent reconstruction of the NAO index. *J. Clim.* 17, 2157–2169.
- Tingley, M.P., Huybers, P., 2009. A Bayesian Algorithm for Reconstructing Climate Anomalies in Space and Time. Part I: Development and Applications to Paleoclimate Reconstruction Problems. *J. Clim.* 23, 2759–2781. <https://doi.org/10.1175/2009JCLI3015.1>
- Trigo, R.M., Valente, M.A., Trigo, I.F., Miranda, P.M.A., Ramos, A.M., Paredes, D., García-Herrera, R., 2008. The Impact of North Atlantic Wind and Cyclone Trends on European Precipitation and Significant Wave Height in the Atlantic. *Ann. N. Y. Acad. Sci.* 1146, 212–234. <https://doi.org/10.1196/annals.1446.014>
- Trouet, V., Esper, J., Graham, N.E., Baker, A., Scourse, J.D., Frank, D.C., 2009. Persistent Positive North Atlantic Oscillation Mode Dominated the Medieval Climate Anomaly. *Science* 324, 78–80. <https://doi.org/10.1126/science.1166349>
- Usoskin, I.G., Gallet, Y., Lopes, F., Kovaltsov, G.A., Hulot, G., 2016. Solar activity during the Holocene: the Hallstatt cycle and its consequence for grand minima and maxima. *Astron. Astrophys.* 587, A150. <https://doi.org/10.1051/0004-6361/201527295>
- Vinther, B.M., Andersen, K.K., Hansen, A.W., Schmith, T., Jones, P.D., 2003. Improving the Gibraltar/Reykjavik NAO index. *Geophys. Res. Lett.* 30. <https://doi.org/10.1029/2003GL018220>
- Wanner, H., Brönnimann, S., Casty, C., Gyalistras, D., Lutherbacher, J., Schmutz, C.J., Stephenson, D.B., Xoplaki, E., 2001. North Atlantic Oscillation - Concepts and studies. *Surv. Geophys.* 22, 321–382. <https://doi.org/10.1023/A:1014217317898>
- Wanner, H., Mercolli, L., Grosjean, M., Ritz, S.P., 2015. Holocene climate variability and change; a data-based review. *J. Geol. Soc.* 172, 254–263. <https://doi.org/10.1144/jgs2013-101>
- Wheeler, D., Garcia-Herrera, R., Wilkinson, C.W., Ward, C., 2010. Atmospheric circulation and storminess derived from Royal Navy logbooks: 1685 to 1750. *Clim. Change* 101, 257–280. <https://doi.org/10.1007/s10584-009-9732-x>
- Williamson, C.E., Saros, J.E., Vincent, W.F., Smol, J.P., 2009. Lakes and reservoirs as sentinels, integrators, and regulators of climate change. *Limnol. Oceanogr.* 54, 2273–2282. [https://doi.org/10.4319/lo.2009.54.6\\_part\\_2.2273](https://doi.org/10.4319/lo.2009.54.6_part_2.2273)
- Woollings, T., Lockwood, M., Masato, G., Bell, C., Gray, L., 2010. Enhanced signature of solar variability in Eurasian winter climate. *Geophys. Res. Lett.* 37. <https://doi.org/10.1029/2010GL044601>
- Zorita, E., González-Rouco, F., 2002. Are temperature-sensitive proxies adequate for North Atlantic Oscillation reconstructions? *Geophys. Res. Lett.* 29, 48–1–48–4. <https://doi.org/10.1029/2002GL015404>

## Supplementary Material

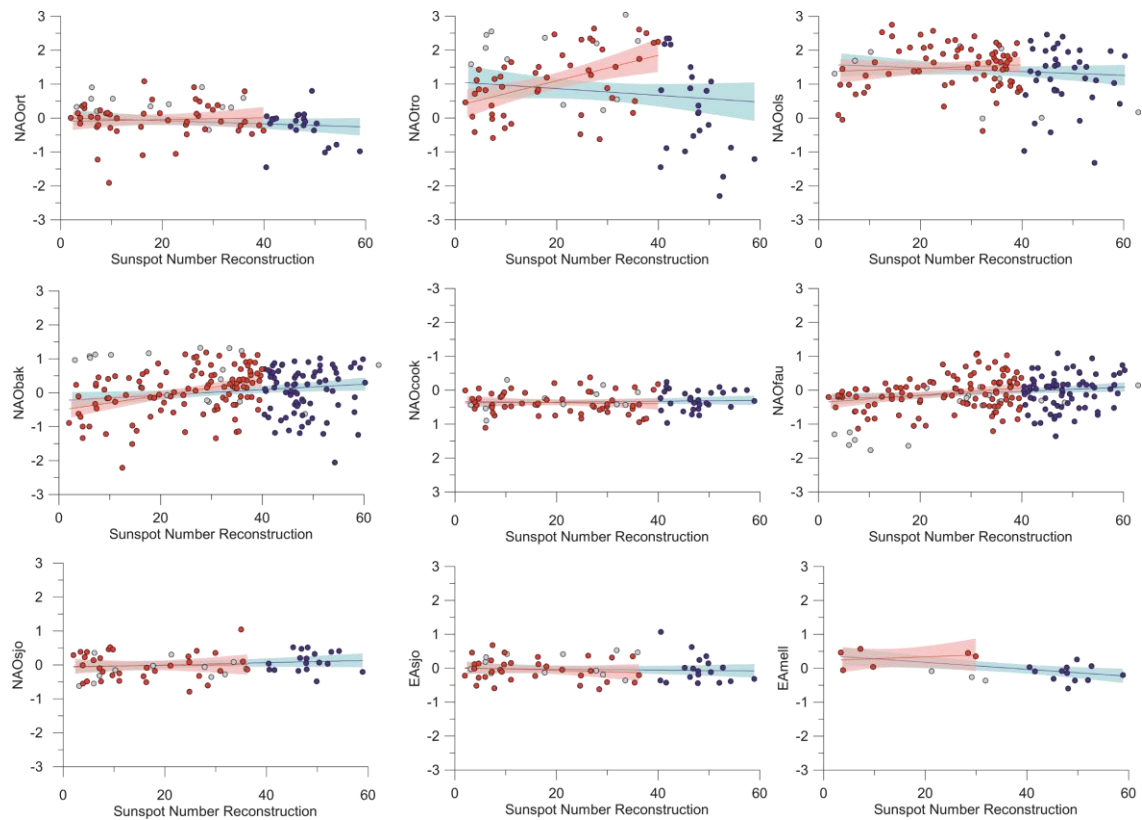


Fig.S1: NAO and EA (right-bottom row) values versus sunspot number reconstruction. Red dots represent samples with sunspot number values below 40, whereas blue dots indicate samples with sunspot number values above 40. Grey dots correspond to samples during decades with high volcanic eruptions; they have not been considered in the correlation analysis. Red line indicates linear correlation between NAO and Sunspot number (< 40) and blue line for all data.

**Table S1: Fifteen global largest volcanic eruptions (according to Sigl et al. 2015) removed from the solar activity analysis**

Year (CE)	Eruption
1815	Tambora (Indonesia)
1809	UE 1809
1783	Laki (Iceland)
1601	Huaynaputina (Peru)
1458	Kuwaae (Vanuatu)
1258	Samalas (Indonesia)
1230	UE 1230
1108	UE 1108
682	Pago? (New Britain)
574	Rabaul? (New Britain)
540	Ilopango? (El Salvador)
536	UE 536
426	UE-426
266	UE 266
44 BCE	Chiltepe? (Nicaragua)